DOI: 10.1021/ma901998r

Macromolecules
ARTICLE

Critical Comparison of Volume Data Obtained by Different Electron Tomography Techniques

Kangbo Lu,[†,§] Erwan Sourty,[†,∥] Ralph Guerra,[⊥] Georg Bar,[#] and Joachim Loos*[,†,‡,§]

[†]*Laboratory of Materials and Interface Chemistry and Soft-Matter CryoTEM Research Unit, and* [‡]*Laboratory of Polymer Technology, Eindhoven University of Technology, PO Box 513, NL-5600 MB Eindhoven, The Netherlands,* [§]*Dutch Polymer Institute, Eindhoven University of Technology, PO Box 902, NL-5600 AX Eindhoven, The Netherlands,* [∥]*FEI Company, Achtseweg Noord 5, Building AAE, 5600 KA Eindhoven/Acht, The Netherlands,* [⊥]*The Dow Chemical Company, Freeport, Texas 77541, and* [#]*Dow Olefinverbund GmbH, PO 1163, 06258 Schkopau, Germany*

Received September 7, 2009; Revised Manuscript Received December 21, 2009

ABSTRACT: We have utilized bright field conventional transmission electron microscopy (BF-CTEM) tomography and annular dark field scanning transmission electron microscopy (ADF-STEM) tomography to characterize a well-defined carbon black (CB) filled polymer nanocomposite with known CB volume concentration. For both imaging methods, contrast can be generated between the CB and the surrounding polymer matrix. The obtained volume reconstructions were analyzed and the CB volume concentrations were carefully determined from the reconstructed data. For both imaging modes the measured CB volume concentrations are substantially different: the CB volume concentration measured in BF-CTEM tomograms exceeds by about 40%, whereas the one measured in ADF-STEM tomograms equals to a good approximation the concentration actually used to synthesize the composite. We critically discuss possible reasons for this significant difference in relation to the characteristics of the imaging technique arguing that, at least in the considered case of low electron scattering materials as polymer systems, ADF-STEM tomography provides good contrast between the components and volume data sets most suitable for further reliable quantification of nanofiller concentrations and filler distributions in polymer nanocomposite systems.

Introduction

Electron tomography provides a mean to reconstruct 3D volumes from TEM specimens with a resolution down to at least one nanometer in the three dimensions.[1,2] Researchers in life sciences have been using transmission electron microscopy (TEM) tomography for more than a decade to obtain three-dimensional volume information on biological structures; more recently, electron tomography has been applied in materials science to characterize the 3D nanostructure of a variety of different materials, too.[3−9] In particular it has been applied intensively to characterize the three-dimensional structure of polymer materials.[10,11] The three-dimensional structural information is reconstructed digitally from a tilt-series of two-dimensional projections. A large number of images projected from the same specimen volume are acquired by tilting the specimen over the maximal achievable tilt range while simultaneously correcting for image shift and focus changes. The tilt-series is then processed off-line using back projection techniques to reconstruct the original volume of the specimen under investigation.[12]

Most tomography studies of polymer systems are based on bright-field conventional transmission electron microscopy (BF-CTEM) tilt-series, mainly relying on phase contrast with a slight underfocus to improve contrast between the polymer components e.g. in block copolymers[10] or blends[13] (possibly after staining the specimens) or the filler and the polymer matrix material. Scanning transmission electron microscopy (STEM) as an incoherent imaging technique[14] is rarely applied for the investigation of polymer systems. In STEM, contrast mainly is achieved by variations of the total elastic scattering cross-section which varies roughly as $Z^{3/2}$ (Z = atomic number). Because polymers mostly consist of carbon and other light elements, STEM imaging is mainly performed on filled or stained systems, where the contrast is created by the Z variations between the filler or staining agent and the polymer matrix, or in case of polymeric multi phase systems, in which an element with higher Z in the polymer chains substantially contributes to the contrast formation, e.g. the Si in PDMS[15−17] or sulfur in ionomers.[18] However, recently we have demonstrated that annular dark field STEM (ADF-STEM) successfully can be applied for imaging even purely carbon-based polymer systems without staining; contrast between the phases is created by their differences in density and to a certain extent their crystalinity.[19]

As stated in ref 19, in particular for the investigation of low electron scattering materials like polymers, and in particular for multiphase systems such as block copolymers, polymer blends or polymer composites filled with carbon nanofillers (e.g., carbon black, carbon nanotubes, or graphene), ADF-STEM imaging and tomography offers several advantages when compared with BF-CTEM. Imaging artifacts inherent to coherent imaging (e.g., Fresnel fringes, contrast reversal, or weak contrast at low spatial frequency) disappear in ADF-STEM[20] and potential staining artifacts are prevented because sufficient contrast is created already without staining.[19] Further, the ADF-STEM signal intensity varies monotically with specimen mass−thickness, therefore fulfilling the so-called "projection criterion".[8]

Modern microscopy provides not only images, volume "images" in case of tomography, but aims at the quantification of the obtained data. This requires that the input data have as little as possible imaging artifacts, which is generally the case with STEM imaging. In the present study we demonstrate the benefit of ADF-STEM tomography for the characterization of polymer

*Corresponding author. E-mail: j.loos@tue.nl.

 Published on Web 01/12/2010

systems. As a specific example a well-defined polymer nanocomposite filled with carbon black (CB) nanoparticles. We demonstrate for our chosen system that ADF-STEM tilt-series provide very reliable input data for further volume quantification of, e.g., filler concentration and distribution.

Experimental Section

The conductive CB filled nanocomposite sample was kindly provided by The Dow Chemical Company. It consists of a polyethylene/polyacryl matrix material (density of 0.92 kg/m^3) and is filled with 16 vol % CB nanoparticles (density of 1.85 kg/m^3). About 100 nm thin specimens were sectioned at cryogenic temperature using a cryo-ultramicrotome (Reichert-Jung Ultracut E, Germany). Subsequently, the thin sections were transferred on a copper TEM grid. Ten different volumes of the sample were analyzed for each imaging technique to provide statistical relevant data.

The BF-CTEM and ADF-STEM experiments here presented were performed on a Titan 80−300 (FEI Company, The Netherlands) equipped with a Fischione 3000 high-angle annular dark field (HAADF) detector at 300 kV acceleration voltage. The detector's "black level" was adjusted by blanking the beam (so that no electron hits the detector) then adjusting the detector offset such that the signal was just a few counts above zero (negligible compared to the detector dynamic range digitized to 16 bits). The detector gain was adjusted after unblanking the beam and making sure all levels of intensity within the scanned image were within the dynamic range of the detector.

All tilt-series were acquired, aligned and reconstructed via the Xplore3D/Inspect3D software suite (FEI Company, The Netherlands). The applied tilting range was always ±70° with tilt angle steps of 1°. The typical dose used over a STEM tilt-series is in the range 10^6 to 10^7 electron/nm^2. Beam damage may be caused locally by long exposure to the beam; more subtle beam damage may cause specimen shrinkage during the tilt-series acquisition.

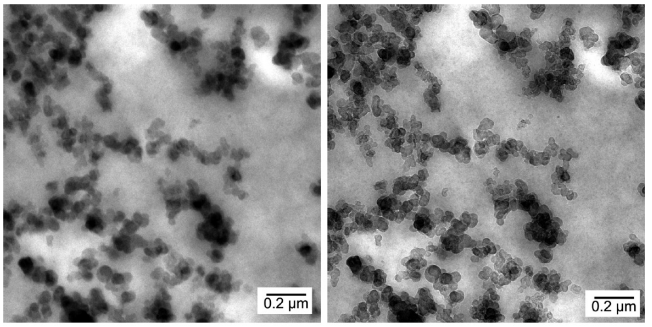

Figure 1. BF CTEM images of the CB nanocomposite acquired for (a) in-focus and (b) slight underfocus conditions.

In the present case, this shrinkage is minimized by pre-exposure to the scanning beam. We are aware that mainly the polymer matrix shrinks, which will increase the relative volume of the CB-phase; however, this principle experimental error accounts for both imaging techniques and was reduced by applying low electron doses. Alignment of the tilt-series was realized with the bead-tracking procedure implemented in Inspect3D. About 20 gold beads were selected and tracked automatically over the entire tilt-series with subsequent manual correction. The bead tracking procedure determines the 3D coordinate of each selected bead in space and compares it to the position of bead projections tracked on each image of the tilt-series. This procedure is iterated five times including optimization of alignment parameters like shift and rotation. The program refines the beads' 3D coordinate between each iteration.[8] The distance in pixels between the projection of the computed 3D coordinate (so-called solution) and the tracked bead position on each image is used to judge the alignment accuracy. The alignment is considered accurate enough when the error averaged over all beads and all images is less than one pixel. The reconstruction algorithm used is SIRT (simultaneous iterative reconstruction technique) with 20 iterations.

Visualization and quantification was done via ResolveRT (Mercury Computer System, FEI Edition). Color rendering was obtained by segmentation: selecting and coloring voxels (3D pixels) of a gray value above a given threshold corresponding to the filler intensity in the reconstructed volume. Volume quantification was performed by surface-rendering and subsequent relating the rendered phase to the whole volume investigated.

Results and Discussion

For our study, we have selected a CB filled conductive nanocomposite, which is an interesting polymer system because understanding of structure−property relations of such "smart" nanocomposite materials is currently a research objective of high importance, mainly focused on specific electrical and mechanical properties. Figure 1 shows images of a selected nanocomposite material acquired in BF-CTEM. The identification of individual CB particles is made difficult due to the lack of contrast when imaging the specimen in focus, only aggregates show strong contrast. In particular, the interface between the CB particles and the polymer matrix appears vague (Figure 1a); however, when operating the BF-CTEM under slight underfocus conditions (−6 μm, which is optimized defocus for the chosen magnification) we are able to substantially increase the contrast between the CB and the surrounding matrix (Figure 1b), which facilitate the identification of individual as well as aggregated CB particles in the polymer matrix.

When applying defocus to increase the contrast we modify the contrast transfer function (CTF) of the TEM optical system such

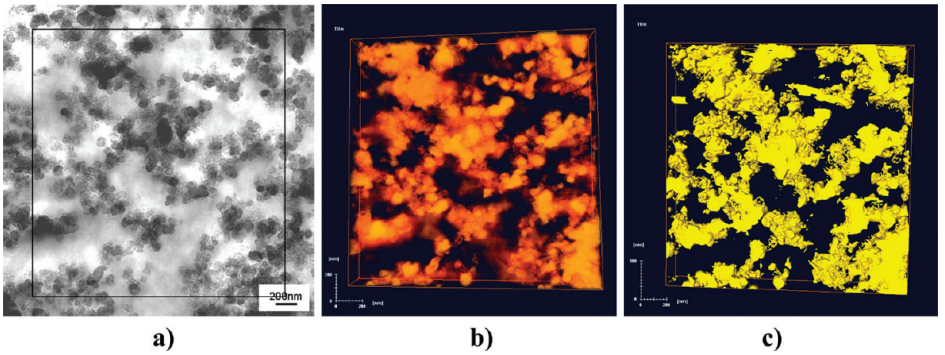

Figure 2. (a) BF-CTEM image of the CB nanocomposite specimen acquired at slight underfocus, the frame indicates about the volume which is reconstructed, (b) corresponding volume reconstruction showing mainly the CB, and (c) surface-rendering of the CB phase.

Table 1. CB Volume Concentrations As Obtained by BF-CTEM and ADF-STEM Tomography Reconstruction[a]

imaging technique	carbon black concentration of 10 different volumes measured per technique (vol %)					average (vol %)	standard deviation (vol %)
BF-CTEM	27.3	19.1	26.6	24.8	27.0	23.6	±3.0
	23.4	21.5	25.2	22.1	18.8		
ADF-STEM	17.4	13.4	17.1	13.3	15.7	15.7	±2.1
	16.2	18.2	11.6	18.3	15.9		

[a] For both imaging modes results of 10 independent measurements are shown and the average volume concentration and standard deviation is calculated.

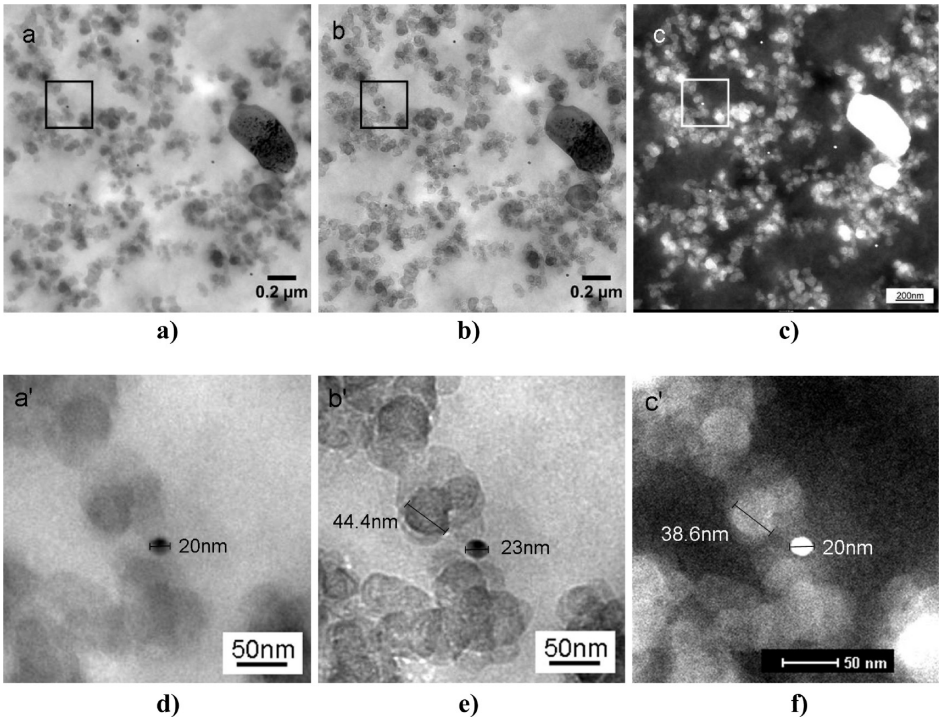

Figure 3. BF-CTEM images of CB particles imbedded in the polymer matrix and a gold bead deposited on the surface of the specimen for (a) in-focus and (b) slight defocus conditions (−1 μm); parts d and e show details of the specimen area which is marked by a frame in parts a and b. (c) ADF-STEM image of the same specimen area as shown in parts a and b and (f) the corresponding high-magnification image. The diameter variations of the gold bead and one CB particle dependent on the imaging conditions applied. The big particle at the right side of parts a−c most probably is an inorganic impurity.

that local variations in specimen density, i.e., local variations of the electron density between CB particles and polymer matrix, induce phase contrast. However, defocusing impacts resolution as effects such as contrast reversal, delocalization, granularity, or Fresnel fringes alter the image contrast.[21] Underfocus is commonly utilized when imaging polymer systems and/or acquiring tilt-series used for tomographic volume reconstruction; the optimum defocus depends on the optical system of the microscope and the applied magnification but always results in creation of similar artifacts.

We have acquired BF-CTEM tilt-series in underfocus over a ±70° tilt range with 1° steps. Figure 2a shows the 0° tilt image of the tilt-series and the frame indicates the area/volume as used for subsequent volume reconstruction. For the chosen imaging conditions distinct contrast between the CB particles and the polymer matrix is obtained. The volume reconstruction is presented in Figure 2b. The features visible in the volume are the CB particles and clusters; the threshold for visualization is set such that the polymer matrix becomes transparent. Some landmarks clearly can be identified both in the original two-dimensional image (Figure 2a) and in the reconstructed volume, which proves that the reconstructed volume correlates with the original tilt series. Because our aim is to determine the volume concentration of the CB in the nanocomposite, the next step is the identification of the CB particles in the reconstructed volume. For this purpose, the so-called iso-surfaces at the interfaces between CB particles and the polymer matrix are created and the CB phase is defined. Figure 2c shows the same volume as in Figure 2b but after surface-rendering and determination of the CB phase. Again, some landmarks easily can be identified in the volume rendering, which proves consistency of our image processing treatments. Because some of the CB particles lay at the surface of the constructed volume, in the iso-surface visualization, such particles appear cut with a closed sectioned surface area (a video file of the tomography reconstructions is available as Supporting Information).

After surface-rendering and determination of the CB volume phase we are able to calculate the volume concentration of the CB phase with respect to the whole reconstructed volume analyzed. In the case of the present data set the CB volume concentration measured is about 23.6 vol %, which exceeds by more than 40% the known 16 vol % CB loading of the sample; some statistical relevant data can be found in Table 1. The definition of the CB phase relies on setting a somewhat subjective threshold between the CB phase and the polymer matrix; however, we have tested the obtained CB volumes by varying systematically the threshold and the results systematically gave a measured CB concentrations significantly too high when applying BF CTEM tomography.

In the following, we would like to discuss the possible origin for the overestimation of the CB volume concentration when quantifying tomographic volume data acquired by BF-CTEM in phase contrast conditions. One possible reason is that imaging in BF-CTEM defocus conditions generates image artifacts like Fresnel fringes, delocalization or granularity, as already described, which in turn cause image distortion. Considering Fresnel fringes formed at an edge, the distance from the edge to the first fringe in proportional to $\sqrt{(\lambda \Delta f)}$, where λ and Δf are respectively the wavelength and defocus.[22] The spherical aberration of the TEM optical system should also contribute to the "delocalization". Figure 3 presents a series of images of the same specimen area obtained in BF-CTEM in focus (Figures 3a/d) and at slight defocus (Figures 3b/e). For the given nanocomposite sample, the electron optical conditions used and the chosen magnification, we selected the defocus such that a balance could be established between visualizing clear interfaces and minimize artifacts. When magnifying the marked area by digitally zooming the image in, the CB filler particles and a gold bead can be identified; however, in case of in-focus imaging, the contrast at the interface between the CB particles and the polymer matrix is very low, making measurement of the exact CB particle diameters practically impossible. Only the gold bead can be distinguished because of its high atomic number and resulting scattering contrast; its diameter is 20 nm.

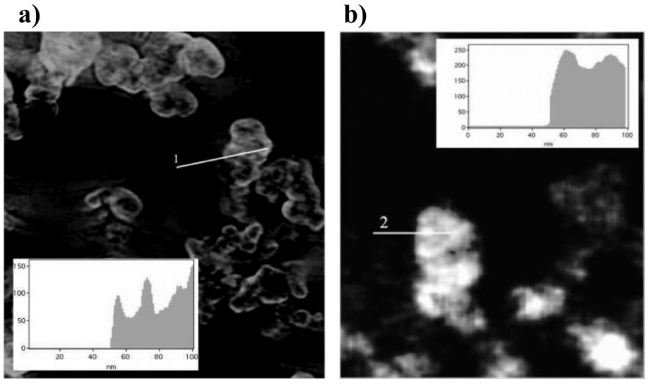

Figure 4. Ortho-slices taken from the (a) BF-CTEM and the (b) ADF-STEM volume reconstructions and the corresponding intensity line profiles (insets) along the indicated lines crossing the interface between polymer matrix and CB particle allowing straightforward assignment of the CB phase and the matrix.

When defocusing, the contrast between the CB particles, the polymer matrix and the gold bead increases (Figure 3, parts b and e). In the magnified image the interface between CB particles and polymer matrix can easily be allocated but image artifacts are also visible. The diameter of a typical CB particle is about 44.5 nm, the diameter of the same gold bead already measured in focus is now about 23 nm, or a 15% increase in diameter.

However, because of the reasonable good contrast between the CB and the surrounding polymer matrix in the tomographic volume data when acquired in BF-CTEM for slight defocus conditions, definition and segmentation of the two phases is straightforward. Figure 4a shows a part of the reconstructed volume before segmentation with high magnification, and the corresponding intensity line profile, which indicates a sharp interface between the CB and the matrix. Similar results for data acquired by ADF-STEM are shown in Figure 4b. These results demonstrate that for both imaging modes binarization has been performed accurately.

For comparison, parts c and f of Figure 3 show corresponding ADF-STEM images of the same specimen area. In a recent study, we have demonstrated that by applying ADF-STEM we see contrast in various (unstained) polymer systems, and we have discussed some specific advantages of ADF-STEM when compared with BF CTEM.[20,21] One observation was that local variations of the density can be utilized to create ADF-STEM images with high contrast and high signal-to-noise ratio even for density differences as low as 0.05 g/cm^3 so that staining, which may cause artifacts, is not needed. Moreover, all images are acquired in focus and formed through incoherent signal collection, which reduces above-mentioned artifacts affecting phase contrast. It was also demonstrated that ADF-STEM is able to image electron beam sensitive polymer crystals so that it could be considered as a kind of low electron dose imaging technique.

In parts c and f of Figure 3, a clear contrast between the CB particles and the polymer matrix is achieved, and in particular measurement of the CB and gold bead diameters can be performed accurately: the diameters of the same CB particle as measured in Figure 3e and the gold bead are 38.5 and 20 nm, respectively. Because ADF-STEM images are acquired in focus, the diameter of the gold bead is equal to that measured in BF-CTEM in focused condition; the diameter of the same CB particle defocused (Figure 3e) is substantially smaller.

In summary, the contrast obtained between the CB particles and the polymer matrix is insufficient to measure the size of the CB particles and clearly distinguish their interfaces with the

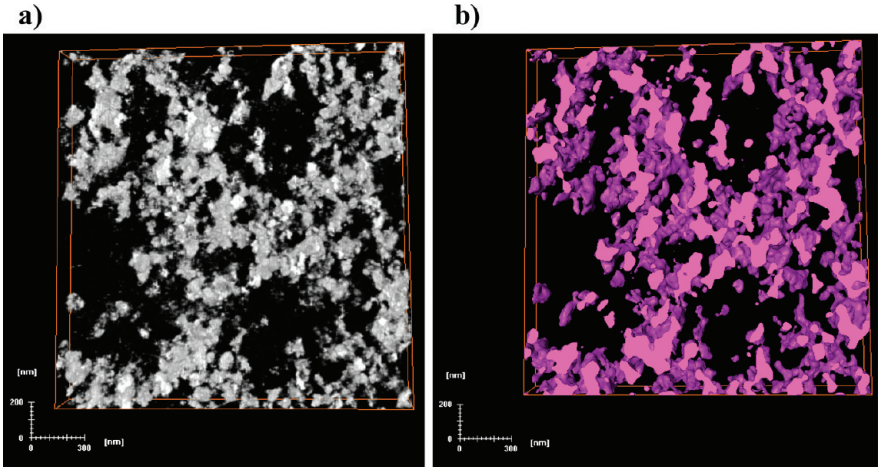

Figure 5. (a) ADF-STEM tomography volume reconstruction showing the CB particles only and (b) the corresponding surface rendering of the CB phase.

polymer matrix when focused in BF-CTEM. The contrast can be increased by defocusing. The diameters of typical features in the few tens nanometer range (corresponding to CB particles and gold beads) are, however, overvalued by about 15% with the defocus used in Figure 3e; the defocus is chosen such that clear contrast between the CB and the polymer matrix is created but imaging artifacts are minimized (actually, the required defocus value depends strongly on the optical system of the microscope and the magnification used). In contrast, ADF-STEM imaging increases the contrast between the CB particles and the polymer matrix and yet allows accurate measurement or the imaged features.

Looking at the tilt-series obtained in BF-CTEM, the corresponding volume reconstruction and CB phase volume calculation, a similar increase in CB particle diameters will result in an increase by more than 40% of the CB volume. Such volume increase is in the same order as the difference between the known CB volume concentration and the one measured from the BF-CTEM tomogram.

Consequently, we have acquired tilt-series of the same CB filled nanocomposite sample by utilizing ADF-STEM, reconstructed the imaged volume (Figure 5a) and defined the CB phase (Figure 5b, (a video file of the tomography reconstructions is available as Supporting Information). As in the case of BF-CTEM tomography, we have acquired 10 different ADF-STEM tilt-series at different sample locations, aligned the images, reconstructed the volume and calculated the average volumes concentration of the CB phase (Table 1). The average CB concentration of 15.7 vol % is close to the specified CB concentration of about 16 vol %. The standard deviation of the CB volume concentration is almost similar for both imaging techniques, reflecting the heterogeneity of the local CB loading within the sample at the scale of the investigated volumes.

Conclusions

We have reconstructed the volume of a carbon black filled conductive polymer nanocomposite by applying BF-CTEM tomography in slight defocus condition and ADF-STEM tomography. After alignment of the tilt-series, volume reconstruction and CB volume phase determination, we have measured average CB volume concentrations and standard deviations for both imaging modes and compared the data with the known CB volume concentration of the nanocomposite. For the BF-CTEM tomography data only defocusing provides enough contrast between the CB particles and the polymer matrix for allocating the CB phase in the tomographic volume reconstruction. However, the average CB volume concentration is much larger than the known concentration. Imaging artifacts and consequent distortion of the particle sizes make the obtained data sets unreliable for further quantification. On the other hand, volume concentration data obtained by ADF-STEM tomography are close to the known CB loading. In both imaging modes, the standard deviation of the CB volume concentration is comparable and reflects the heterogeneity of the sample under investigation at the length scale we have observed. In summary, ADF-STEM imaging is able to create good contrast between different phases in polymer systems without the need of staining and it introduces fewer artifacts because of its incoherent nature so that volume data sets based on this imaging technique are very reliable for further quantification. Potential applications of ADF-STEM investigations can be found in the research fields of block copolymers, polymer blends, or polymers composites filled with low electron scattering nanoparticles such as the CB discussed in this study, carbon nanotubes or graphene, to name but a few.

Acknowledgment. The work forms part of the Dutch Polymer Institute (DPI) research program. Additional financial support was provided by the Dutch Science Organization (NWO). Further, we like to thank Bob Vastenhout from Dow Benelux B. V., Terneuzen, The Netherlands, for his help with microtoming the highly filled samples.

Supporting Information Available: Movies showing the tomography reconstructions. This material is available free of charge via the Internet at http://pubs.acs.org.

References and Notes

(1) De Rosier, D. J.; Klug, A. *Nature* **1968**, *217*, 130.
(2) Bonetta, L. *Nat. Methods* **2005**, *2*, 139.
(3) Weyland, M.; Yates, T. J. V.; Dunin-Borkowski, R. E.; Laffont, L.; Midgley, P. A. *Scr. Mater.* **2006**, *55*, 29.
(4) Weyland, M.; Midgley, P. A. *Mater. Today* **2004**, *7*, 32.
(5) Koster, A. J.; Chen, H.; Sedat, J. W.; Agard, D. A. *Ultramicroscopy* **1992**, *46*, 207.
(6) Koster, A. J.; Ziese, U.; Verkleij, A. J.; Janssen, A. H.; De Jong, K. P. *J. Phys. Chem. B* **2000**, *104*, 9368.
(7) Midgley, P. A.; Weyland, M. *Ultramicroscopy* **2003**, *96*, 413.
(8) Kübel, C.; Voigt, A.; Schoenmakers, R.; Otten, M.; Su, D.; Lee, T.-C.; Carlsson, A.; Bradley, J. *Microsc. Microanal.* **2005**, *11*, 378.
(9) Möbus, G.; Inkson, B. J. *Mater. Today* **2007**, *10*, 18.
(10) Jinnai, H.; Spontak, R. J. *Polymer* **2009**, *50*, 1067.
(11) Midgley, P. A.; Ward, E. P. W.; Hungría, A. B.; Thomas, J. M. *Chem. Soc. Rev.* **2007**, *36*, 1477.
(12) Frank, J. *Electron Tomography: Three-dimensional Imaging with the Transmission Electron Microscope*; Plenum Press: New York, 1992.
(13) Sengupta, P.; Noordermeer, J. W. M. *Macromol. Rapid Commun.* **2005**, *26*, 542.
(14) Nellist, P. D.; Pennycook, S. J. *Ultramicroscopy* **1999**, *78*, 111.
(15) Drummy, L. F.; Wang, Y. C.; Schoenmakers, R.; May, K.; Jackson, M.; Koerner, H.; Farmer, B. L.; Mauryama, B.; Vaia, R. A. *Macromolecules* **2008**, *41*, 2135.
(16) Kim, G.; Sousa, A.; Meyers, D.; Libera, M. *Microsc. Microanal.* **2008**, *14*, 459.
(17) Benetatos, N. M.; Chan, C. D.; Winey, K. I. *Macromolecules* **2007**, *40*, 1081.
(18) Zhou, N. C.; Chan, C. D.; Winey, K. I. *Macromolecules* **2008**, *41*, 6134.
(19) Loos, J.; Sourty, E.; Lu, K.; de With, G.; van Bavel, S. *Macromolecules* **2009**, *42*, 2582.
(20) Sourty, E.; van Bavel, S.; Lu, K.; Guerra, R.; Bar, G.; Loos, J. *Microsc. Microanal.* **2009**, *15*, 251.
(21) Reimer, L. Kohl, H. *Transmission Electron Microscopy: Physics of Image Formation*, 5th ed.; Springer-Verlag: New York, 2008; p 188.
(22) Williams, D. B.; Carter, C. B. *Transmission Electron Microscopy*; Plenum Press: New York, 1996.